CrossMark
←click for updates

Amphiphilic graphene oxide stabilisation of hexagonal BN and MoS$_2$ sheets†

M. Haniff Wahid,[ab] Xianjue Chen,*[a] Christopher T. Gibson[a] and Colin L. Raston*[a]

A simple and scalable method has been developed for directly forming water-dispersible van der Waals solids involving mixing aqueous solution of graphene oxide (GO) with hexagonal boron nitride (BN) or molybdenum disulphide (MoS$_2$) in *N*-methylpyrrolidone. The GO acts as an amphiphile in stabilising the colloidal solutions of the heterolaminar material in water.

The breakthrough in unveiling the exceptional properties of graphene has triggered extensive research efforts in two-dimensional (2D) materials, including inorganic layered analogues such as hexagonal boron nitride (BN), and molybdenum disulfide (MoS$_2$), and other transition metal dichalcogenides, and layered oxides.[1] In addition to investigating the behaviour of monolayers, there is a rapidly emerging focus on constructing or reassembling isolated layers of such material into designer multi-layer heterostructures that are bound together primarily by van der Waals forces.[2] Such cohesion forces essentially preserve the distinct electronic properties of individual layers of the material,[3] enabling tunable properties of the heterostructures, with potential for functioning as high performance electronic switches and optoelectronic devices that are still challenging to access for graphene due to the absence of an intrinsic energy bandgap.[4]

Advancing the practical applications of the above heterolaminar van der Waals materials requires the development of scalable syntheses. In comparison to the well-developed strategies for fabricating graphene and quasi-graphene forms (graphene oxide or reduced graphene oxide), the possibility of making multi-layer van der Waals solids has only recently been achieved experimentally.[5,6] Significant efforts have been made towards growing graphene, monolayer BN and MoS$_2$ epitaxially on top of each other with controllable quality, although finding the right

conditions for growing continuous layers is challenging.[7–9] Another approach is layer-by-layer deposition from 2D material suspensions *via* Langmuir–Blodgett techniques.[10,11] It is also possible to mix preformed colloidal suspensions of different 2D materials to generate layered flocculates.[12] This solution-based self-organising method is versatile and scalable, showing promise for producing van der Waals solids as ultrathin dielectrics,[10] selectively permeable membranes,[13] and composite materials.[14] However, there are some limitations on the present approaches which involve the use of specific organic solvents that have similar surface tension to that of the stabilised 2D materials.[15,16] Organic solvents can only ensure temporary stability and finite concentration of the 2D material suspensions,[17] and thus can restrict further processing of such materials. It is also difficult to produce stabilised inorganic lamellar materials, including BN and MoS$_2$, in aqueous media in the absence of additional surfactants due to their hydrophobic property.[18,19] Indeed access to water-processable quasi-graphene forms such as graphene oxide and reduced graphene oxide has dramatically advanced the potential of graphene-based materials into much broader areas.[20,21] Hence, there is significant scope for developing novel and versatile solution-based protocols to prepare water-dispersible heterolaminar van der Waals materials.

In this work we develop the use of graphene oxide (GO) sheets as both the composite material and the surfactant for supporting and stabilising BN and MoS$_2$ sheets in water. GO is amphiphilic due to the presence of carboxyl and hydroxyl groups at the edges and hydrophobic unoxidized polyaromatic islands within the basal plane.[22,23] This amphiphilic property has been used for effectively stabilising pristine graphite flakes and carbon nanotubes,[23] creating highly stable Pickering emulsions,[23,24] and constructing three-dimensional networks of GO hollow spheres.[25] This suggests that GO is capable of non-covalently assembling with BN or MoS$_2$ sheets *via* van der Waals interactions and/or hydrophobic effects, at the same time stabilising the heterolaminar materials in water, and this is the focus of the work reported herein.

The overall procedure for preparing the heterolaminar materials is summarised in Fig. 1. GO was prepared from high

[a] Centre for NanoScale Science and Technology, School of Chemical and Physical Sciences, Flinders University, Bedford Park, SA 5042, Australia.
  E-mail: colin.raston@finders.edu.au; Tel: +61 88201 7958
[b] Department of Chemistry, Faculty of Science, Universiti Putra Malaysia, 43400 Serdang, Selangor, Malaysia

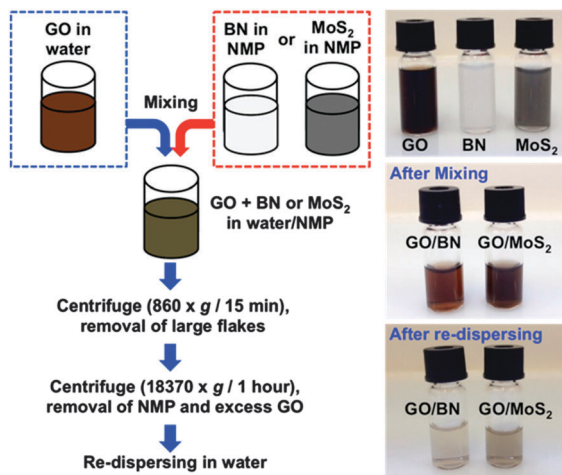† Electronic supplementary information (ESI) available. See DOI: 10.1039/c5cc02066b

Fig. 1 Schematic illustration of the sample preparation and corresponding photographs of the resulting dispersions.

purity graphite flakes powder (99.9%, SP-1, Bay Carbon) using the modified Hummer's method.‡[26,27] Colloidal dispersions (10 mL) of BN (1 mg mL^{-1}) and MoS$_2$ (1 mg mL^{-1}) in N-methylpyrrolidone (NMP) were prepared using probe sonication for 1 hour. Each dispersion was then diluted to 0.2 mg mL^{-1} (0.5 mL) and directly added drop-wise into 0.5 mL of colloidal suspension of GO (0.5 mg mL^{-1}), followed by mild sonication for 30 seconds. The stability of the suspensions were investigated under acidic (pH 1), neutral and basic (pH 12) conditions. We selected a relatively low starting concentration for BN and MoS$_2$ dispersions, because higher concentrations were observed to induce instability of the mixed solutions, presumably due to an increase in irreversible loading of BN or MoS$_2$ sheets onto GO sheets. The resulting mixed dispersions were centrifuged (860 $\times$ g, 15 min) to remove any large flakes of the starting laminar materials, with the supernatants then separated, affording the colloidal dispersions of GO–BN and GO–MoS$_2$. Centrifugation of samples prepared under acidic condition showed complete precipitation, and thus loss of stability of the material (ESI-S1†). NMP was the dispersing medium of choice for the exfoliation and stabilization due to the insolubility of BN and MoS$_2$ in water, but not in NMP, as well as the infinite miscibility of NMP with water. Despite the ability to directly exfoliate BN and MoS$_2$ in the presence of GO, pre-sonication of BN and MoS$_2$ in NMP effectively avoids any risk of damaging the structure of GO. The NMP in the resulting solutions can be further removed by centrifugal-washing the samples at 18 370 $\times$ g for 1 hour, and redispersing the sediments into water, affording stable dispersions, Fig. 1. The colour difference between the solutions after mixing and after re-dispersing arises from the higher stability of the GO devoid of BN or MoS$_2$, whereas the heterolaminar materials are more readily separated centrifugally.

Control experiments involving mixing NMP solutions of BN and MoS$_2$ with water showed no evidence for forming stable dispersions, clearly establishing that the formation of any dispersions in water requires the presence of GO. This supports our hypothesis that GO acts as an amphiphilic surfactant, in binding to BN and MoS$_2$ through the hydrophobic islands in

lowering their interfacial energy, with hydrophilic groups on the outer surface of the GO stabilising the colloidal dispersion of the heterolaminar material in water. Pertaining to the effect of pH, under acidic conditions there is a loss in stability of the GO (ESI-S1†) whereas stable dispersions formed under neutral and basic (pH 12) conditions. The electrostatic stability of the re-dispersed solutions of GO–BN and GO–MoS$_2$ at neutral pH was confirmed by zeta potentials, at −48.3 mV, −47.7 mV and −50.3 mV, respectively, for GO solution, and re-dispersed solutions of GO–BN and GO–MoS$_2$.

Transmission electron microscopy (TEM) was used to investigate the state of the re-dispersed composite materials in water, by dropping dispersions onto a holey carbon coated copper grid and drying under ambient conditions. TEM images for pristine GO, exfoliated BN and MoS$_2$ are shown in Fig. 2a–d, respectively. Graphene oxide sheets ($\sim$200 nm to 10 μm in lateral dimensions) are evident in Fig. 2a and 3a, with the corresponding electron diffraction (inset) revealing a typical pattern for monolayers. The pattern rings of electron diffraction in the inset of Fig. 2b are consistent with randomly stacked layers of GO.[28] TEM images and corresponding electron diffraction patterns from selected areas in Fig. 2c and d, for as prepared separate NMP solutions of BN and MoS$_2$, confirm the presence of exfoliated BN and MoS$_2$ sheets. The exfoliated sheets range in size from $\sim$200 nm to 1 μm for both materials. While BN gives a similar shape and size due to the smaller cross section of the starting material ($\sim$1 μm), MoS$_2$ ($\sim$2 μm) shows an apparent fragmentation, presumably arising from high energy cavitation processes associated with the sonication and less strong in-plane stiffness compared with BN sheets.[29] Fig. 2e and g show the composites of GO–BN and GO–MoS$_2$ in the re-dispersed solutions, respectively, with the size of the BN and MoS$_2$ consistent with that of the as-exfoliated sheets in NMP. Similar images were obtained for samples prepared under basic conditions (ESI-S2†). The electron diffraction pattern in Fig. 2f is similar to that of the stacking monolayers in Fig. 2b. Even though it is difficult to determine the overlapping diffraction spots of BN in this pattern, as BN and graphene have very similar crystal structures with a lattice constant difference of $\sim$2%, the difference in contrast, size and shape of BN and GO sheets provides a means to recognise BN. In the case of GO–MoS$_2$, the electron diffraction (Fig. 2h) shows a typical pattern for MoS$_2$, along with the GO ring pattern. The TEM analysis also shows that BN and MoS$_2$ always accompany GO, which is in accordance with the BN and MoS$_2$ sheets being supported on the surface of GO in the re-dispersed solutions.

Atomic force microscopy (AFM) was undertaken to further investigate the morphology of the heterolaminar materials. The pristine GO is monolayered having a measured thickness of $\sim$1 nm,[21] Fig. 3a and b. The structures of heterolaminar materials are consistent with TEM analysis, with BN and MoS$_2$ supported on GO evident in Fig. 3c, e and f. The height profile measurement in Fig. 3d along the orange line in Fig. 3c reveals a thickness of $\sim$5 nm for BN. The height profiles for the GO–MoS$_2$ show that the sheets of MoS$_2$ are $\sim$8–12 nm thick, Fig. 3g. The difference in thickness is related to the different interplanar distances between BN ($\sim$0.33 nm) and MoS$_2$ ($\sim$0.61 nm), as well as the higher surface energy of MoS$_2$ ($>$250 mJ m^{-2}) compared
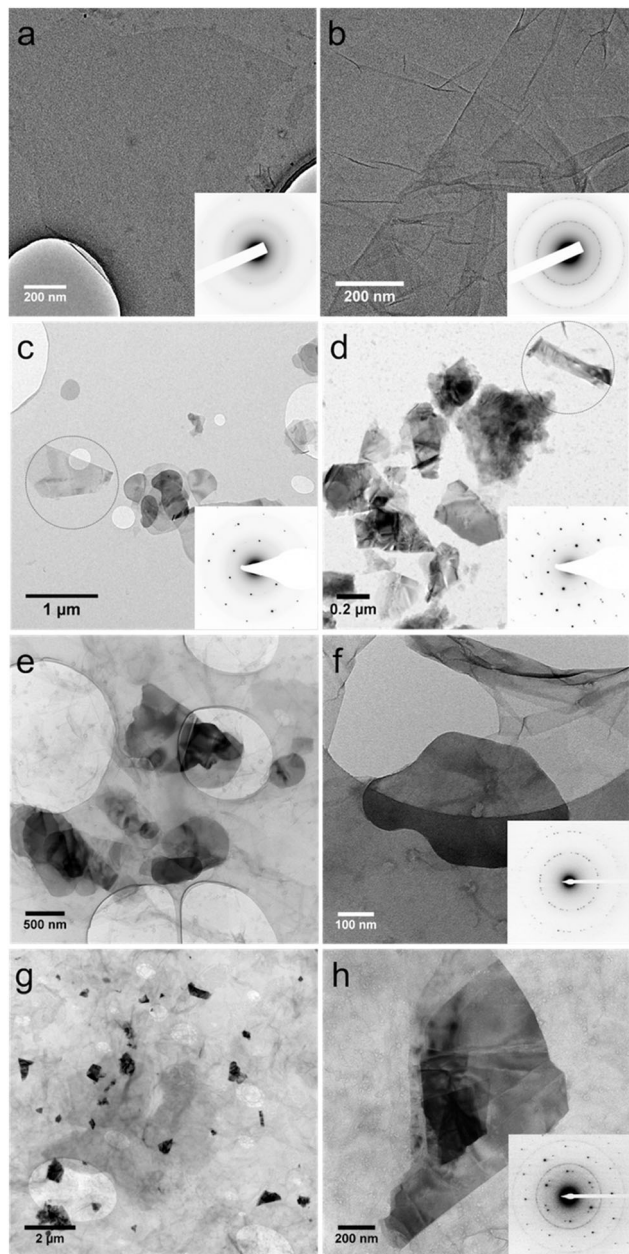
Fig. 2 TEM images of (a, b) GO, (c) exfoliated BN and (d) MoS$_2$ sheets, (e, f) GO–BN and (g, h) GO–MoS$_2$. Electron diffraction patterns for all samples are as shown in the inset.
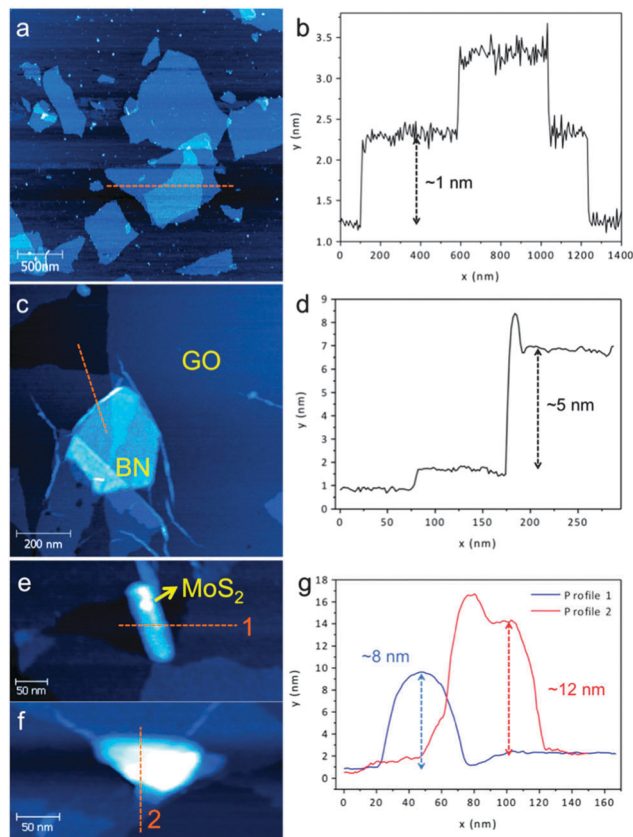

Fig. 3 AFM images and height profiles of the indicated area in (a, b) GO, (c, d) GO–BN, and (e, f, g) MoS$_2$ samples.
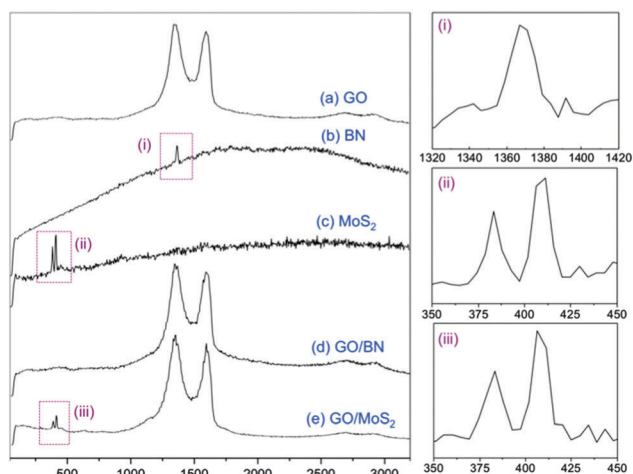

Fig. 4 Raman spectra of pristine (a) GO, (b) BN, (c) MoS$_2$ and composite material of (d) GO–BN and (e) GO–MoS$_2$, respectively. Zoomed-in images of the peaks labelled as (i), (ii) and (iii) are shown on the right.

to that of BN ($\sim$110 mJ m^{-2}),[30,31] requiring higher energy input for exfoliation.

Raman spectra were recorded for pristine GO, BN and MoS$_2$, and for the re-dispersed heterolaminar materials respectively (Fig. 4). Typical spectra for GO displayed a D and G band at $\sim$1370 cm^{-1} and $\sim$1570 cm^{-1} respectively (Fig. 4a).[32] For BN (Fig. 4b) and MoS$_2$ (Fig. 4c), strong fluorescence background was observed, possibly due to the remaining NMP which was used as the dispersant. BN exhibits a characteristic peak at $\sim$1360 cm^{-1} that is due to the E$_{2g}$ phonon mode which is similar to the G peak in graphitic materials, as shown in the zoomed-in image in Fig. 4(i).[33] MoS$_2$ has characteristic peaks at

$\sim$380 cm^{-1} and $\sim$400 cm^{-1} which are attributed to the E$_{2g}^1$ and A$_{1g}$ modes, respectively, Fig. 4(ii).[34] Strong D and G bands for GO are evident for both GO–BN and GO–MoS$_2$. The characteristic peak for BN cannot be seen due to overlap with the strong D band for GO, whereas for MoS$_2$, both characteristic peaks are discernible, Fig. 4(iii).

In conclusion, we have developed a facile method for preparing heterolaminar van der Waals composites based on graphene oxide and BN or MoS₂ in water. This involves a simple sonication of BN and MoS₂ in NMP as a dispersing medium, for then adding to preformed GO in water, with the subsequent processing leading to aqueous solutions devoid of organic solvent. Importantly the method can be readily scaled into gram quantities of the material. Moreover, this work extends the utility of GO in stabilising 2D layered materials in water and consequently it opens up new facile processing adventures for 2D layered materials in general, particularly in water.

Notes and references

‡ *Methods summary*: GO used in this study was prepared from natural graphite flakes powder (99.9%, SP-1, Bay Carbon) using the modified Hummer's method.[26,27] Probe sonication was carried out using a Vibra-Cell™ VCX130 sonicator at 60% amplitude for all samples. Centrifugations were performed using the Dynamica Velocity 14R. Zeta potential analysis was performed using a Malvern Zetasizer Nano series. Measurements for each sample were recorded in triplicate and 20 data acquisitions were recorded in each measurement. All measurements were recorded at 25 °C in Malvern disposable clear Folded Capillary Cells. TEM samples were prepared by depositing a drop of the suspension onto a holey carbon coated copper grid (#2450-AB, SPI Supplies) and dried under ambient conditions. TEM analysis was carried out using a Philips CM200 instrument operating at 120–200 kV. Image J software was used for processing all the TEM images. Raman spectra were acquired using a Witec alpha300R Raman microscope with excitation laser wavelength of 532 nm (≤5 mW), at room temperature. The spectra were recorded with an ×40 objective (Numerical Aperture 0.60) for each sample with typical integrations times between 10 to 20 seconds with 3 accumulations per spectrum. Atomic force microscopy (AFM) analysis in tapping mode was performed with a Bruker multimode AFM and a NanoScope V under ambient conditions. AFM probes used were Mikromasch HQ:NSC15 Si probes with a nominal spring constant of 40 N m⁻¹ and a nominal tip diameter of 16 nm. The AFM scanner was calibrated in the x, y and z axes using Si calibration grids (Bruker model numbers PG: 1 μm pitch, 110 nm depth, and VGRP: 10 μm pitch, 180 nm depth). Samples were deposited on mica substrates and dried in air prior to analysis.

1 A. K. Geim and K. S. Novoselov, *Nat. Mater.*, 2007, **6**, 183.
2 A. K. Geim and I. V. Grigorieva, *Nature*, 2013, **499**, 419.
3 B. Radisavljevic and A. Kis, *Nat. Mater.*, 2013, **12**, 815.
4 G. S. Duesberg, *Nat. Mater.*, 2014, **13**, 1075.
5 C. R. Dean, A. F. Young, I. Meric, C. Lee, L. Wang, S. Sorgenfrei, K. Watanabe, T. Taniguchi, P. Kim, K. L. Shepard and J. Hone, *Nat. Nanotechnol.*, 2010, **5**, 722.
6 L. A. Ponomarenko, A. K. Geim, A. A. Zhukov, R. Jalil, S. V. Morozov, K. S. Novoselov, I. V. Grigorieva, E. H. Hill, V. V. Cheianov, V. I. Fal'co, K. Watanabe, T. Taniguchi and R. V. Gorbachev, *Nat. Phys.*, 2011, **7**, 958.
7 T. Tanaka, A. Ito, A. Tajiima, E. Rokuta and C. Oshima, *Surf. Rev. Lett.*, 2003, **10**, 721.
8 Z. Liu, L. Song, S. Zhao, J. Huang, L. Ma, J. Zhang, J. Lou and P. K. Ajayan, *Nano Lett.*, 2011, **11**, 2032.
9 Y. Shi, W. Zhou, A.-Y. Lu, W. Fang, Y.-H. Lee, A. L. Hsu, S. M. Kim, K. K. Kim, H. Y. Yang, L.-J. Li, J.-C. Idrobo and J. Kong, *Nano Lett.*, 2012, **12**, 2784.
10 M. Osada and T. Sasaki, *Adv. Mater.*, 2012, **24**, 210.
11 K. Ariga, Q. Ji, J. P. Hill, Y. Bando and M. Aono, *NPG Asia Mater.*, 2012, **4**, e17.
12 G. Gao, W. Gao, E. Cannuccia, J. Taha-Tijerina, L. Balicas, A. Mathkar, T. N. Narayanan, Z. Liu, B. K. Gupta, J. Peng, Y. Yin, A. Rubio and P. K. Ajayan, *Nano Lett.*, 2012, **12**, 3518.
13 R. R. Nair, H. A. Wu, P. N. Jayaram, I. V. Grigorieva and A. K. Geim, *Science*, 2012, **335**, 442.
14 R. J. Young, I. A. Kinloch, L. Gong and K. S. Novoselov, *Compos. Sci. Technol.*, 2012, **72**, 1459.
15 Y. Hernandez, V. Nicolosi, M. Lotya, F. M. Blighe, Z. Sun, S. De, I. T. McGovern, B. Holland, M. Byrne, Y. K. Gun'ko, J. J. Boland, P. Niraj, G. Duesberg, S. Krishnamurthy, R. Goodhue, J. Hutchison, V. Scardaci, A. C. Ferrari and J. N. Coleman, *Nat. Nanotechnol.*, 2008, **3**, 563.
16 J. N. Coleman, M. Lotya, A. O'Neill, S. D. Bergin, P. J. King, U. Khan, K. Young, A. Gaucher, S. De, R. J. Smith, I. V. Shvets, S. K. Arora, G. Stanton, H.-Y. Kim, K. Lee, G. T. Kim, G. S. Duesberg, T. Hallam, J. J. Boland, J. J. Wang, J. F. Donegan, J. C. Grunlan, G. Moriarty, A. Shmeliov, R. J. Nicholls, J. M. Perkins, E. M. Grieveson, K. Theuwissen, D. W. McComb, P. D. Nellist and V. Nicolosi, *Science*, 2011, **331**, 568.
17 W. W. Liu and J. N. Wang, *Chem. Commun.*, 2011, **47**, 6888.
18 X. Chen, R. A. Boulos, P. K. Eggers and C. L. Raston, *Chem. Commun.*, 2012, **48**, 11407.
19 X. Chen, W. Zang, K. Vimalanathan, K. S. Iyer and C. L. Raston, *Chem. Commun.*, 2013, **49**, 1160.
20 Y. Si and E. T. Samulski, *Nano Lett.*, 2008, **8**, 1679.
21 D. Li, M. B. Müller, S. Gilje, R. B. Kaner and G. G. Wallace, *Nat. Nanotechnol.*, 2008, **3**, 101.
22 D. R. Dreyer, S. Park, C. W. Bielawski and R. S. Ruoff, *Chem. Soc. Rev.*, 2010, **39**, 228.
23 J. Kim, L. J. Cote, F. Kim, W. Yuan, K. R. Shull and J. Huang, *J. Am. Chem. Soc.*, 2010, **132**, 8180.
24 S. C. Thickett and P. B. Zetterlund, *ACS Macro Lett.*, 2013, **2**, 630.
25 X. Chen, P. K. Eggers, A. D. Slattery, S. G. Ogden and C. L. Raston, *J. Colloid Interface Sci.*, 2014, **430**, 174.
26 W. S. Hummers and R. E. Offeman, *J. Am. Chem. Soc.*, 1958, **80**, 1339.
27 N. I. Kovtyukhova, P. J. Ollivier, B. R. Martin, T. E. Mallouk, S. A. Chizhik, E. V. Buzaneva and A. D. Gorchinskiy, *Chem. Mater.*, 1999, **11**, 771.
28 J.-K. Lee, S. Lee, Y.-I. Kim, J.-G. Kim, B.-K. Min, K.-I. Lee, Y. Park and P. John, *Sci. Rep.*, 2014, **4**, 5682.
29 C. Ataca, H. Şahin, E. Aktürk and S. Ciraci, *J. Phys. Chem. C*, 2011, **115**, 3934.
30 K. Weiss and J. M. Philips, *Phys. Rev. B: Solid State*, 1976, **14**, 5392.
31 K. M. Knowles and S. Turan, *Cryst. Res. Technol.*, 2000, **35**, 751.
32 S. Stankovich, D. A. Dikin, R. D. Piner, K. A. Kohlhaas, A. Kleinhammes, Y. Jia, Y. Wu, S. T. Nguyen and R. S. Ruoff, *Carbon*, 2007, **45**, 1558.
33 R. V. Gorbachev, I. Riaz, R. R. Nair, R. Jalil, L. Britnell, B. D. Belle, E. W. Hill, K. S. Novoselov, K. Watanabe, T. Taniguchi, A. K. Geim and P. Blake, *Small*, 2011, **7**, 465.
34 C. Lee, H. Yan, L. E. Brus, T. F. Heinz, J. Hone and S. Ryu, *ACS Nano*, 2010, **4**, 2695.